Targeting GLUT1 in acute myeloid leukemia to overcome cytarabine resistance

Hannah Åbacka,[1] Jesper S. Hansen,[1] Peng Huang,[1] Raminta Venskutonytė,[1] Axel Hyrenius-Wittsten,[2] Giulio Poli,[3] Tiziano Tuccinardi,[3] Carlotta Granchi,[3] Filippo Minutolo,[3] Anna K. Hagström-Andersson[2] and Karin Lindkvist-Petersson[1,4]

[1]Department of Experimental Medical Science, Medical Structural Biology, BMC C13, Lund University, Lund, Sweden; [2]Department of Laboratory Medicine, Division of Clinical Genetics, BMC C13, Lund University, Lund, Sweden; [3]Department of Pharmacy, University of Pisa, Pisa, Italy and [4]LINXS - Lund Institute of Advanced Neutron and X-ray Science, Scheelevägen 19, SE-223 70, Lund, Sweden

Correspondence: KARIN LINDKVIST-PETERSSON - karin.lindkvist@med.lu.se

Supplementary material for

Targeting GLUT1 in acute myeloid leukemia to overcome Cytarabine resistance

Supplementary Methods

GLUT inhibitor assay measured in giant vesicles

Giant vesicles reconstituted with protein were prepared by gentle hydrogel swelling (1). Inhibitor effects on GLUT1-facilitated glucose uptake were measured using our previously published Amplex Red reporter assay (2). The detailed step-by-step protocol has also been made available (3). The inhibitors as indicated were used at a concentration of 30 μM and glucose transport was initiated by adding 4 mM D-glucose to the inhibitor equilibrated (5 min) giant vesicles. Data are presented as mean + SD from n = 5 number of experiments.

Molecular docking

PGL-14 was built using Maestro (4) and then minimized into a water environment with Macromodel (5) (employing the generalized Born/surface area model). The minimization was performed using conjugate gradient, the MMFFs force field and a distance-dependent dielectric constant of 1.0, until a convergence value of 0.05 kcal/(Å·mol) was reached. PGL-14 was docked into the recently deposited structure of the glucose transporter GLUT1 in the inward-open state, complexed with a phenylalanine amide inhibitor (PDB code 5EQG) (6) reusing AUTODOCK4.2 (7). AUTODOCK TOOLS (8) were employed to define the torsion angles in the ligand, to add the solvent model and to assign partial atomic charges (Gasteiger for the ligands and Kollman for the receptors). The ligand was docked into the central cavity of GLUT1 occupied by the inhibitor. The docking site was defined considering the bound ligand as the central group of a grid of 52, 66, and 58 points in the x, y, and z directions, respectively. The energetic map calculations were carried out by using a grid spacing of 0.375 Å and a distance-

dependent function of the dielectric constant. The ligand was subjected to 200 runs of the AUTODOCK search using the Lamarckian genetic algorithm with 10'000'000 steps of energy evaluation; the number of individuals in the initial population was set to 500 and a maximum of 10'000'000 generations were simulated during each docking run. All other settings were left as their defaults. For each docking site, the clusters of solutions with a population higher than 10 %, i.e. including more than 10 % of all the generated docking poses were taken into account, for a total of three different clusters.

Molecular dynamic simulations

All molecular dynamic (MD) simulations were performed with AMBER 16 (9) employing the ff14SB force field following a validated protocol already used in pose prediction studies (10, 11). General Amber force field (GAFF) parameters were assigned to the ligands, while partial charges were calculated using the AM1-BCC method as implemented in the Antechamber suite of AMBER 16. The four GLUT1/PGL-14 complexes were placed in a parallelepiped water box using the TIP3P explicit solvent model. Chloride ions were added as counter ions for the neutralization of the systems. A step of energy minimization, consisting of 5000 steps of steepest descent followed by conjugated gradient, were performed on the solvated complexes before running the MD simulations. These were carried out using Particle mesh Ewald electrostatics and periodic boundary conditions, a cutoff of 10 Å for the nonbonded interactions and a time step of 2.0 fs, since all bonds involving hydrogen atoms were kept rigid using SHAKE algorithm. The minimized systems were subjected to an initial MD step of 0.5 ns performed with constant-volume periodic boundary conditions, during which the temperature of the system was raised from 0 to 300 K. A following constant-pressure periodic boundary MD was then performed for 3 ns to allow the equilibration of the system, in which the temperature was kept at the constant value of 300 K using the Langevin thermostat. Eventually,

an MD production step of 26.5 ns was performed with constant pressure and temperature conditions, for a total simulation time of 30 ns.

Binding energy evaluations

Ligand-protein binding energy evaluations were performed as already reported (12, 13) using AMBER 16. The trajectories relative to the last 15 ns of MD simulations generated for the GLUT1/PGL-14 complexes were employed for the calculations, for a total of 150 snapshots (at time intervals of 100 ps). The gas and water phases of the systems were represented using dielectric constants of 1 and 80, respectively. Van der Waals, electrostatic, and internal interactions were calculated with the SANDER module of AMBER 16. Polar energies were calculated using the Poisson-Boltzmann method with the MM-PBSA module of AMBER 16, while nonpolar energies were estimated using the MOLSURF program.

GLUT inhibitor binding measured by intrinsic fluorescence quenching

Binding of inhibitors to GLUT1 was measured by tryptophan quenching as published (14). Briefly, purified protein was mixed with inhibitor dissolved in DMSO. The protein was diluted to a final concentration of 0.25 mg/mL GLUT1. The protein-ligand mixture was then transferred to a 70 μL quartz fluorometer cell and equilibrated for 5 min at 20 °C before recording the spectrum. Fluorescence spectra were recorded using a Jasco J-810 spectropolarimeter equipped with FMO-427S fluorescence module. The excitation wavelength was 295 nm and emission spectra were recorded between 310 and 400 nm. The background of the reagents alone without protein was subtracted individually for all recorded protein fluorescence spectra and baselines were adjusted. For both PGL-13 and PGL-14 spectra up to 600 μM final concentration of the compound were recorded, however the 600 μM result was deemed to be not reliable due to tendency of PGLs to precipitate after mixing with protein sample or buffer at higher concentrations and is therefore not presented here.

Cell culture

AML cell lines THP-1, KG-1, Monomac-6 (MM6) and OCI-AML-3 were all purchased from DSMZ (Braunschweig, Germany). They were maintained in Gibco™ RPMI 1640 (Thermo Fisher Scientific) supplemented with 10 % fetal bovine serum (FBS) and 1 % penicillin/streptomycin in 37 °C, 5 % CO_2.

Microscopy

THP-1 and KG-1 cells in a PBS with 2 % FBS suspension were spun down onto microscopy slides and fixed in 4 % PFA (10 min, RT) followed by permeabilization with PBS-Tween20 (0.25 % Tween-20, 10 min, RT). After being washed in PBS-Tween20 (0.1 % Tween-20) and subsequent blocking with 1 % BSA for 1 h in RT the slides were incubated with primary antibody against GLUT1 (1:500, Abcam ab15309) at 4 °C overnight. After another washing step, the slides were incubated with an Alexa Fluor® 568 conjugated secondary antibody (1:1000, Abcam ab175470) and DAPI (1 µg/mL, Merck) for 1 h at room temperature. After washing, the slides were mounted using an antifade mountant (Life Technologies). Images were obtained using a Nikon A1 plus confocal microscope (Nikon Instruments) and NIS-elements, version: 4.50.02, (Laboratory Imaging).

Western blot

AML cell line pellets were lysed for 10 minutes at 4 °C in a tube rotator in Tris-HCl (50 mM, pH 7.4), 50 µM sodium orthovanadate, 5 mM sodium pyrophosphate, 1 mM EGTA, 1 mM EDTA, 270 mM sucrose, NP-40 (1 % w/v), 1 mM DTT, 50 mM NaF and cOmplete™ protease inhibitor cocktail (Merck). Cell debris was removed by centrifugation (14000 xg, 15 min, 4 °C) followed by collection of the supernatant. Protein concentration was determined using the Bicinchoninic Acid Protein Assay Kit (Merck). Cell lysate proteins were separated by a 4-12 % Bis-Tris gel followed by blotting onto a nitrocellulose membrane using semi-dry transfer.

The membrane was blocked in skim milk (10 % w/v, 30 min, RT) followed by incubation with primary antibodies against GLUT1 (1:1000, Abcam ab15309) and GAPDH (1:1000, Santa Cruz Biotechnology sc-47724) overnight at 4 °C. After washing in TBS-Tween20 (0.1 % Tween-20) the membrane was incubated with HRP conjugated secondary antibodies (1:5000, Invitrogen 31460 and 1:5000, GE Healthcare NA9310V) for 1 hour at RT. The protein signal was developed using SuperSignal™ West Pico Plus Chemiluminiscent Substrate (Thermo Scientific). GLUT1 bands were compared to GAPDH control bands using ImageJ (Vers. 1.52d). Trans-membrane proteins commonly show a "smeared" appearance on gels as we also see here for GLUT1, differences in molecular weight are also often detected potentially depending on the level of glycosylation's or other post translation modifications that may vary depending on host cell.

Viability assay

Cytarabine (Ara-C) and Doxorubicin were obtained from Selleckchem (Houston, TX, USA) and diluted in NaCl to stock solutions of 20 mg/mL and 0.6 mg/mL for Ara-C and Doxorubicin, respectively. Brequinar sodium salt hydrate and maltose monohydrate were purchased from Merck. The day before each experiment, AML cells were split to 0.5×10^6 cells/mL in 2/3 fresh and 1/3 conditioned media. Cells were seeded in white luminescence 96-well plates at 50 μL with 25 000 cells/well. PGL-13, PGL-14, Ara-C, Doxorubicin and Brequinar were diluted in DMSO (Merck) to 1000x stock solutions followed by several dilution steps in cell media. Lastly, 50 μL of the drug dilutions were added to the wells in triplicate-quintuplicate, reaching a final volume of 100 μL/well with a maximum of 0.3 % DMSO (0.1-0.3 %). Maltose was directly diluted in cell media before added to wells. Drug concentrations were ranging from 137-100000 nM (PGL-13), 137-500000 nM (PGL-14), 11.43-25000 nM (Ara-C), 1.42-1035 nM (Doxorubicin), 0.98-1000 mM (maltose) and 0.64-10000 nM (Brequinar). Cell viability was determined after 72 hours of incubation (37 °C, 5 % CO) by the luminescent cell viability

assay CellTiter-Glo® 2.0 (Promega, Madison, WI, USA) according to manufacturer's instructions. Briefly, the plate was equilibrated in RT for 30 min after which 100 μL CellTiter-Glo® 2.0 reagent was added to each well. The samples were mixed on a shaker (2 min, RT, 300 rpm) and equilibrated for 10 min at RT. Luminescence was recorded using Veritas™ Microplate Luminometer (Turner biosystems, Sunnyvale, CA, USA). The percentage of inhibition in viability was determined by calculating the reduction in luminescence levels for wells treated with drugs compared to DMSO-treated negative control wells as in the following formula: $100 - \left[100 \times \left(\frac{luminescence\ (drug)}{mean\ luminescence\ (negative\ control)}\right)\right]$. The concentration of DMSO in the control was always the same within each experiment, thus when three drugs were combined each drug combination had 3x the DMSO. Half maximal inhibitory concentrations (IC_{50}) and suboptimal concentrations (equivalent to 25 % inhibition, IC_{25}) were calculated using GraphPad Prism 7.04 (La Jolla, CA, USA). For the assay of maltose together with Ara-C, both maltose and Ara-C were directly diluted in cell media and wells containing only media were used as negative controls. For combinatorial treatments drugs were added to cells at the IC_{25} concentration alone or in combination. If the IC value was negative, indicative of a pipetting error, that individual well was removed from the calculations of the average, never leaving less than three values to calculate the average effect of IC.

Calculations of synergy.

Synergistic effect from co-treatments was calculated using the Bliss Independence model (15). With this method drug effects are measured as probabilities ($0 \geq P \leq 1$) of drug independence. Shortly, combination index (CI) was calculated using the formula $CI = \frac{E_A + E_B + \cdots + E_N - E_A E_B - E_A E_N - E_B E_N - \cdots - E_A E_B \ldots E_N}{E_{AB \ldots N}}$ where the inhibitory effect of N number of drugs are analysed. The effect of all drugs combined ($E_A + E_B + E_N$) are calculated taken their predicted additive effect ($E_A E_B$ etc.) into consideration. This effect is then compared to the

observed combinatory effect ($E_{AB...N}$). When CI < 1 the co-treatment effect was considered

synergistic. If CI ≥ 1 the effect was assigned not synergistic, hence having additive or no effect.
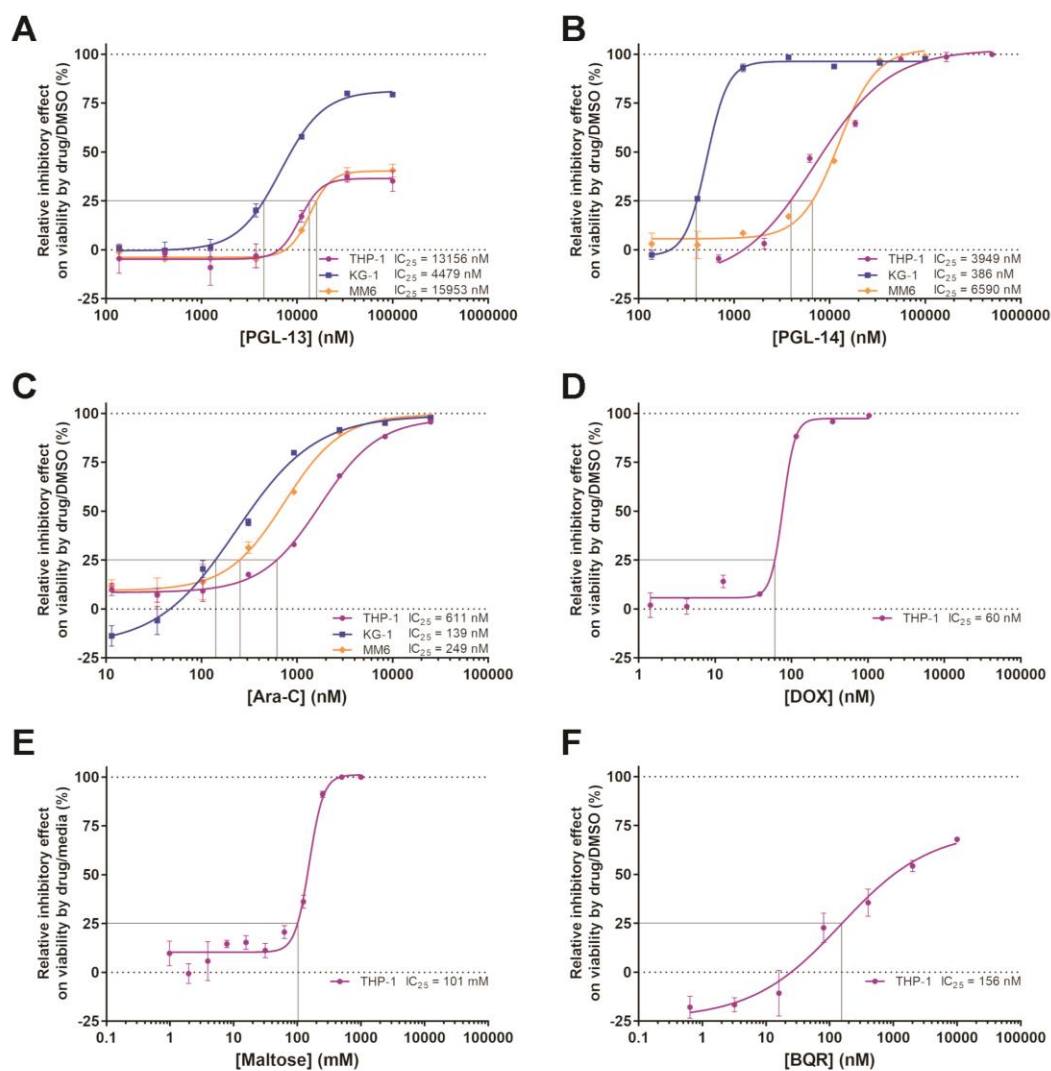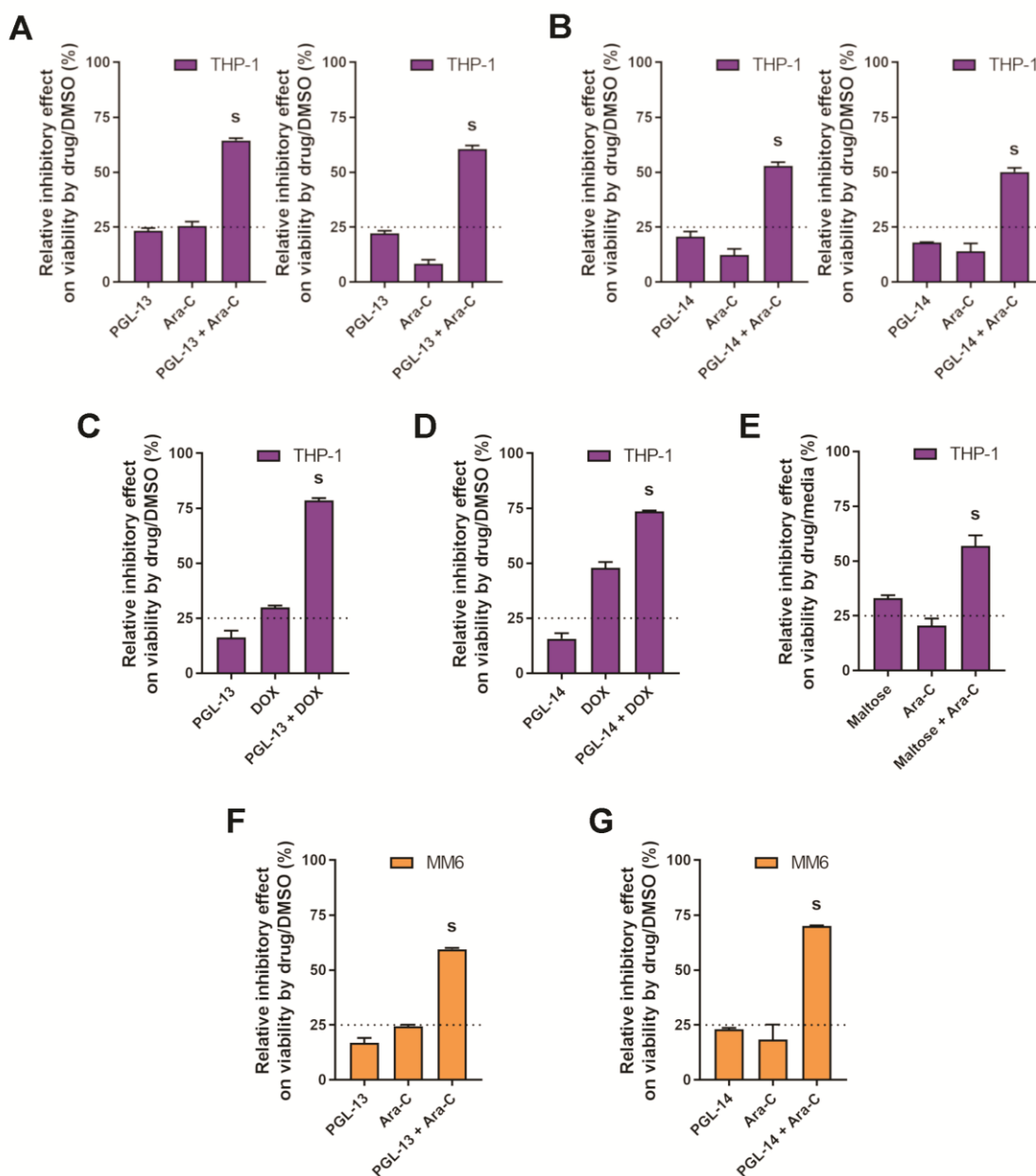
Supplementary figures
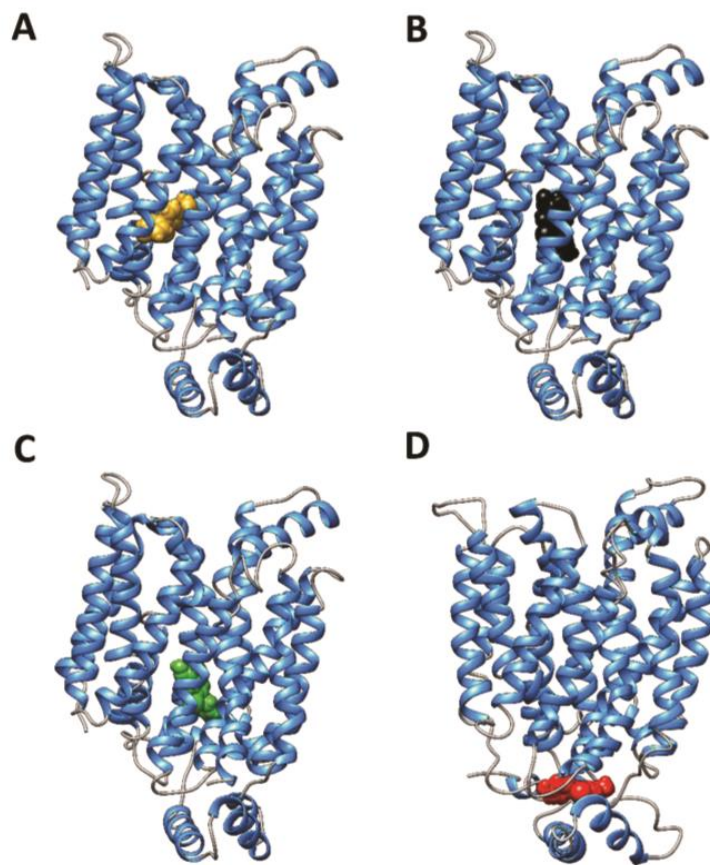
Supplementary Figure 1. The four GLUT1-PGL-14 complexes studied with MD simulations are shown. In (a) complex 1, (b) complex 2, (c) complex 3 and (d) complex 4, PGL-14 is shown as spheres and colored in gold, black, green and red, respectively. GLUT1 is shown as blue cartoon for all complexes.
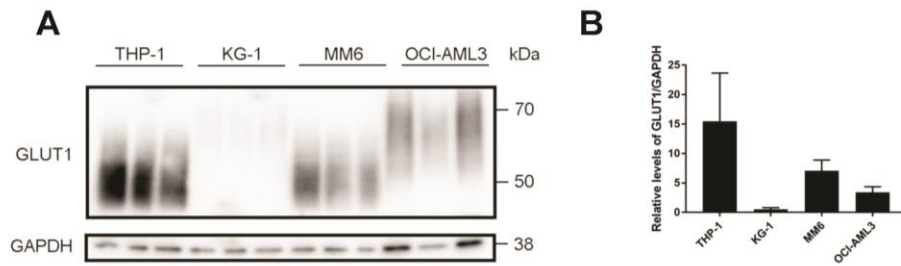
Supplementary Figure 2. Western blot of AML cell lines showing GLUT1 expression levels. (a) THP-1, KG-1, MM6 and OCI-AML-3 whole lysates showing expression levels of GLUT1 with GAPDH as loading control. (b) Relative amounts of GLUT1 compared to GAPDH. Bars show mean + SD, n = 3.

Supplementary Figure 3. Relative inhibitory effect on THP-1 (magenta), KG-1 (blue) and MM6 (orange) cells for different concentrations of GLUT1 inhibitors (a) PGL-13 and (b) PGL-14, as well as for chemo drugs (c) cytarabine (Ara-C) and (d) Doxorubicin (DOX) along with disaccharide (e) maltose and DHODH inhibitor (f) Brequinar (BQR). Lines highlight IC_{25} values, which also are displayed for every compound used. Values show mean + SD, n = 3.

Supplementary Figure. 4. Synergistic co-treatment effects by drugs and inhibitors in THP-1 (magenta) and MM6 (orange) cells. (a) Two repeated analyses of PGL-13 inhibition of cell viability in co-treatments with Ara-C. Combination index (CI) values are (left) 0.67 and (right) 0.47. (b) Two repeated measurements of co-treatment effect by PGL-14 and Ara-C with CI values of (left) 0.58 and (right) 0.59. (c) Inhibitory effect by PGL-13 together with Doxorubicin, CI = 0.53. (d) Inhibition with PGL-14 and Doxorubicin, CI = 0.76. (e) Co-treatment effect by maltose and Ara-C, CI = 0.82. (f) Inhibition by PGL-13 and Ara-C, CI = 0.62. (g) Inhibition by PGL-14 and Ara-C, CI = 0.53. Values were compared to DMSO or media control. Bars show mean + SD, n = 3. Drugs were used at IC_{25} concentrations and synergistic effects have been marked with [S].
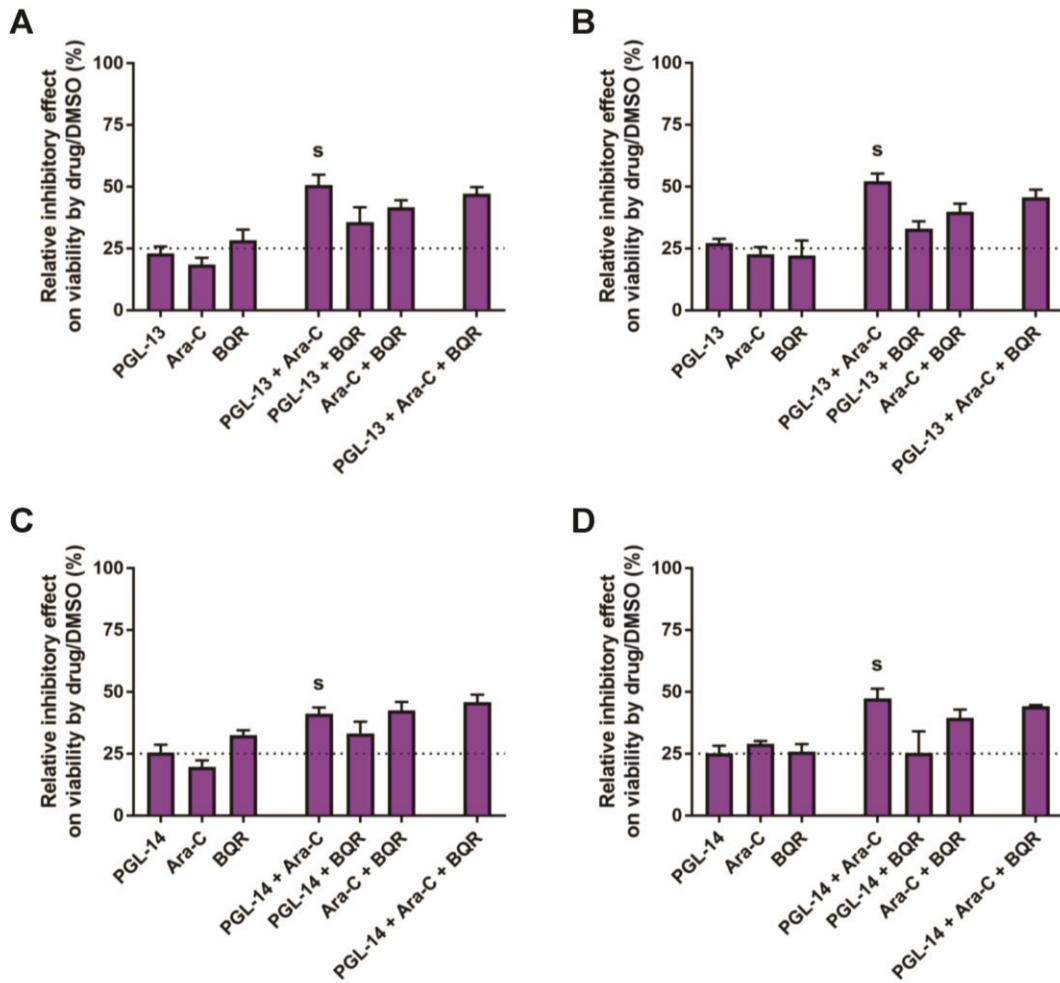
Supplementary Figure. 5. Inhibitory effect by PGLs and Brequinar (BQR) in co-treatment with Ara-C in THP-1 cells. Inhibition by PGLs, Ara-C and Brequinar alone, and in co-treatment with two drugs combined as well as with all three drugs combined. Results for PGL-13 (a) CI = 0.73, (b) CI = 0.84 and equivalent combination therapies with PGL-14 (c) CI = 0.98, (d) CI = 0.99 showed similar findings. Bars show mean + SD compared to DMSO control, n = 3-5. All drugs were added at IC$_{25}$ concentrations and synergistic effects are marked with ^{S}.

Supplementary references

1.	Hansen JS, Thompson JR, Helix-Nielsen C, Malmstadt N. Lipid directed intrinsic membrane protein segregation. J Am Chem Soc. 2013;135(46):17294-17297.
2.	Hansen JS, Elbing K, Thompson JR, Malmstadt N, Lindkvist-Petersson K. Glucose transport machinery reconstituted in cell models. Chemical communications. 2015;51(12):2316-2319.
3.	Hansen JS, Lindkvist-Petersson K. Glucose Transport Activity Measured in Giant Vesicles. Methods in molecular biology. 2018;1713:77-91.
4.	Maestro, version 9.0; Schrödinger Inc: Portland, OR. 2009.
5.	Macromodel, version 9.7; Schrödinger Inc: Portland, OR. 2009.
6.	Kapoor K, Finer-Moore JS, Pedersen BP, et al. Mechanism of inhibition of human glucose transporter GLUT1 is conserved between cytochalasin B and phenylalanine amides. Proc Natl Acad Sci U S A. 2016;113(17):4711-4716.
7.	Morris GM, Huey R, Lindstrom W, et al. AutoDock4 and AutoDockTools4: Automated docking with selective receptor flexibility. J Comput Chem. 2009;30(16):2785-2791.
8.	Sanner MF. Python: a programming language for software integration and development. J Mol Graph Model. 1999;17(1):57-61.
9.	Case D.A. BV, Berryman J.T. , Betz R.M. , etal. AMBER 14, University of California, San Francisco. 2014.
10.	Dal Piaz F, Vera Saltos MB, Franceschelli S, et al. Drug Affinity Responsive Target Stability (DARTS) Identifies Laurifolioside as a New Clathrin Heavy Chain Modulator. J Nat Prod. 2016;79(10):2681-2692.
11.	Poli G, Lapillo M, Jha V, et al. Computationally driven discovery of phenyl(piperazin-1-yl)methanone derivatives as reversible monoacylglycerol lipase (MAGL) inhibitors. J Enzyme Inhib Med Chem. 2019;34(1):589-596.
12.	Granchi C, Caligiuri I, Bertelli E, et al. Development of terphenyl-2-methyloxazol-5(4H)-one derivatives as selective reversible MAGL inhibitors. J Enzyme Inhib Med Chem. 2017;32(1):1240-1252.
13.	Tuccinardi T, Manetti F, Schenone S, Martinelli A, Botta M. Construction and validation of a RET TK catalytic domain by homology modeling. J Chem Inf Model. 2007;47(2):644-655.
14.	Kraft TE, Hresko RC, Hruz PW. Expression, purification, and functional characterization of the insulin-responsive facilitative glucose transporter GLUT4. Protein Sci. 2015;24(12):2008-2019.
15.	Foucquier J, Guedj M. Analysis of drug combinations: current methodological landscape. Pharmacol Res Perspect. 2015;3(3):e00149.